Key Points:
- Arctic Ocean freshwater content in a fully coupled climate model has a memory of at least a decade of previous atmospheric forcing
- Observed changes in Arctic Ocean freshwater content over recent decades can be explained by sea-level pressure variations
- Long memory suggests potential for predictability

Supporting Information:
- Supporting Information S1

Correspondence to:
H. L. Johnson,
helen.johnson@earth.ox.ac.uk

Arctic Ocean Freshwater Content and Its Decadal Memory of Sea-Level Pressure

Helen L. Johnson[1] [iD], **Sam B. Cornish[1]** [iD], **Yavor Kostov[2]** [iD], **Emma Beer[3]** [iD], and **Camille Lique[4]** [iD]

[1]Department of Earth Sciences, University of Oxford, Oxford, UK, [2]Department of Physics, University of Oxford, Oxford, UK, [3]Scripps Institution of Oceanography, University of California San Diego, La Jolla, CA, USA, [4]Laboratoire d'Océanographie Physique et Spatiale, UMR6523, Ifremer-CNRS-UBO-IRD, Brest, France

Abstract Arctic freshwater content (FWC) has increased significantly over the last two decades, with potential future implications for the Atlantic meridional overturning circulation downstream. We investigate the relationship between Arctic FWC and atmospheric circulation in the control run of a coupled climate model. Multiple linear lagged regression is used to extract the response of total Arctic FWC to a hypothetical step increase in the principal components of sea-level pressure. The results demonstrate that the FWC adjusts on a decadal timescale, consistent with the idea that wind-driven ocean dynamics and eddies determine the response of Arctic Ocean circulation and properties to a change in surface forcing, as suggested by idealized models and theory. Convolving the response of FWC to a change in sea-level pressure with historical sea-level pressure variations reveals that the recent observed increase in Arctic FWC is related to natural variations in sea-level pressure.

Plain Language Summary This paper shows that the Arctic Ocean circulation and freshwater storage in a fully coupled climate model have a long memory of atmospheric conditions, adjusting to a change in sea-level pressure over more than a decade. This is important because the Arctic Ocean has recently accumulated a large amount of freshwater, which may ultimately be exported to the Atlantic, with implications for the circulation and heat transport there, yet we do not know if or when it will be exported and at what rate. Based on the relationship we deduce between sea-level pressure and Arctic freshwater content, we estimate changes in Arctic freshwater content over the last century and show that observed changes since 1992 can largely be explained by historical changes in the winds driving the ocean circulation. Our results have implications for the attribution of Arctic variability and change, the interpretation of observational and model data, and the prediction of freshwater export to the North Atlantic.

1. Introduction

The Arctic region is warming twice as fast as the global mean (Intergovernmental Panel on Climate Change, 2013), and its summer sea-ice extent has reduced by approximately 50% since satellite measurements began in 1979 (Vihma, 2014). There have also been significant subsurface changes in the Arctic Ocean. Between 1992 and 2012, the Arctic accumulated an additional 12,000 km³ of liquid freshwater (Rabe et al., 2014), most of it in the Beaufort Gyre (Proshutinsky et al., 2009). This recently accumulated freshwater may ultimately exit the Arctic and flow into the North Atlantic; large freshwater fluxes from the Arctic to the North Atlantic have been observed in the past (e.g., Belkin et al., 1998) and are likely to be more pronounced if they follow a period of accumulation. Changes in the export of freshwater from the Arctic Ocean have the potential to significantly influence global ocean circulation and climate via their impact on the salinity of the North Atlantic dense water formation regions and the Atlantic meridional overturning circulation (e.g., Jahn & Holland, 2013; Stouffer et al., 2006).

It is now well established from observations and numerical models that the liquid freshwater content (FWC) of the Arctic Ocean's largest freshwater reservoir, the Beaufort Gyre, varies on seasonal to decadal timescales (e.g., Proshutinsky & Johnson, 1997). On interannual timescales, this variability is thought to be related principally to changes in ocean surface stress, which depends on the wind forcing but is modulated by sea-ice conditions (e.g., Giles et al., 2012; Proshutinsky et al., 2009). When the anticyclonic surface stress over the

Beaufort Gyre is intensified, freshwater accumulates through Ekman convergence and subsequent down-welling, deepening the halocline in the center of the Beaufort Gyre and steepening isopycnals (Proshutinsky et al., 2009), spinning up the gyre. Recent observational studies suggest that for at least some of the year, despite an anticyclonic atmospheric circulation, surface ocean velocities match or exceed those of the sea-ice, which hence acts as a drag on the circulation (Dewey et al., 2018; Meneghello et al., 2018). Nevertheless, on average the anticyclonic winds result in Ekman convergence.

In idealized models and theory, this process is arrested by baroclinic eddies; isopycnal slopes increase until eddies (resolved or parameterized) are able to bring the system into equilibrium, such that the FWC of the Beaufort Gyre is sustained by a balance between Ekman convergence and an eddy-induced volume transport towards the boundary (Davis et al., 2014; Lique et al., 2015; Manucharyan & Spall, 2016). After a change in surface stress, the FWC in these models comes into equilibrium on decadal timescales, determined by the eddy diffusivity. Eddies are ubiquitous in the limited observations we have of the Arctic (e.g., Zhao et al., 2016), although their formation regions and mechanisms are poorly pinned down.

In this manuscript we isolate the time-dependent relationship between atmospheric circulation and Arctic FWC in a more realistic, fully coupled, climate model simulation with the added complexity of bathymetry, sea-ice and coupled processes. To do this we determine the amplitude and timescale of the response of total Arctic FWC to a step change in sea-level pressure, that is, the "climate response function" (CRF). Because much of the Arctic's freshwater, and its variability, is associated with the Beaufort Gyre, this is related to the spin-up timescale of the gyre. However, variability in total Arctic FWC, which is what matters for export to the Atlantic (Haine et al., 2015; Jahn et al., 2010; Lique et al., 2009), also depends on the dynamics governing the Trans-polar Drift, as well as freshwater storage over the shelves and exchange with the interior. The redistribution mechanisms within the Arctic are less well understood (Carmack et al., 2016).

Rather than performing a model perturbation experiment in which the coupling between the atmosphere and ocean is somehow modified (see the complementary ocean-sea-ice model experiments described in Marshall et al., 2017), we use multiple lagged regression in an existing long control run to extract the linear response of integrated Arctic FWC to a hypothetical step change in surface forcing. This diagnostic Green's function approach is particularly useful because, if the relationship is linear, the response function can be convolved with a time series of forcing to reconstruct FWC variability.

2. Model Details and Methodology

We analyze monthly mean output from a 150-year control integration performed with the High-Resolution Global Environmental Model (HiGEM). HiGEM is a fully coupled climate model based on the Hadley Centre Global Environmental Model version 1 (HadGEM1; Johns et al., 2006) with a relatively high resolution ocean and a reasonable representation of the Arctic (Lique et al., 2015, 2017). The model is described and evaluated in Shaffrey et al. (2009). It uses a spherical latitude-longitude grid with an atmospheric horizontal resolution of 0.83° latitude by 1.25° longitude (N144) and 38 vertical levels, and an oceanic resolution of 1/3° by 1/3° with 40 unevenly spaced vertical levels. In the ocean, the lateral mixing of tracers is parameterized using the isopycnal formulation of Griffies et al. (1998) with constant isopycnal diffusivity; there is also a scale-selective biharmonic scheme for the momentum dissipation, and a biharmonic scheme to represent enhanced mixing of temperature and salinity in the upper 20 m. Eddies are permitted at mid- to low latitudes but parameterized at high latitudes by the biharmonic version (Roberts & Marshall, 1998) of the Gent and McWilliams (1990) adiabatic mixing scheme with a latitudinally varying thickness diffusion coefficient. The sea-ice model is based on the Community Ice Code (CICE; Hunke & Dukowicz, 1997) and uses an elastic-viscous-plastic rheology with a five-category ice thickness distribution.

The atmosphere and ocean are initialized from rest using data from the European Centre for Medium-Range Weather Forecasting analysis and the World Ocean Atlas 2001 (Boyer et al., 2005), respectively. In this control integration greenhouse gases are held constant at late 20th-century concentrations (345 ppm for CO_2) and there is no source of external forcing, such that all climate anomalies can be attributed to internal variability. We disregard the first 20 years, during which there is a significant spin-up in FWC; some small model drift remains (see Figure 1a).

We follow the approach of Kostov et al. (2017) to determine the response of Arctic FWC in the HiGEM control integration to a step change in atmospheric forcing. We first define an index of integrated FWC, relative to a
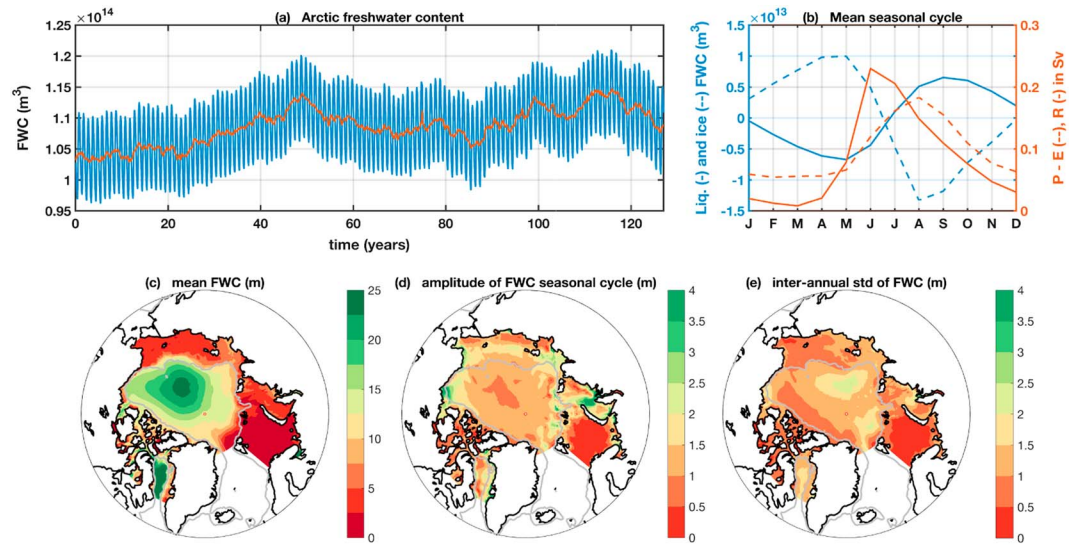
Figure 1. (a) Time series of freshwater content (FWC; relative to a salinity of 34.8, integrated over the Arctic basin and down to the 34.8 isohaline). Monthly mean values are plotted in blue, and the time series with mean seasonal cycle removed is shown in red. (b) Mean seasonal cycle in Arctic liquid FWC (solid blue line) and sea-ice (dashed blue line), snowfall plus precipitation minus evaporation (red dashed line) and river runoff (solid red line). Spatial distribution of the (c) mean FWC, (d) amplitude of the mean seasonal cycle, and (e) standard deviation after mean seasonal cycle removed (m).

reference salinity $S_{ref} = 34.8$ (Aagaard & Carmack, 1989) and integrated down to the 34.8 isohaline over the entire Arctic domain shown in Figure 1c:

$$FWC = \int \int \int_{z(S=S_{ref})}^{0} \frac{S_{ref} - S}{S_{ref}} \, dV \qquad (1)$$

We characterize the variability in surface forcing over the Arctic using the first three empirical orthogonal functions (EOFs) of the sea-level pressure field (mean seasonal cycle removed) north of 70°N and their principal component time series (see section 4). Following Hasselmann et al. (1993), we then consider the FWC time series as the convolution of an impulse response function G (a Green's function) with the previous history of atmospheric forcing:

$$FWC(t) = \int_0^{\tau_{max}} G(\tau)PC(t-\tau) \, d\tau + \epsilon(t) \qquad (2)$$

where $PC(t)$ is one of the principal components of sea-level pressure, normalized by its standard deviation, τ is the time lag, τ_{max} is an imposed maximum cutoff lag, $\epsilon(t)$ is residual noise, and $G(\tau)$ represents the time-dependent response to an impulse perturbation of magnitude one standard deviation in PC.

We discretize (in steps of 1 month) and estimate the impulse response function $G(\tau)$ by multiple linear least squares regression of the detrended FWC signal against the lagged PC index. When performing the regression, we divide the PC time series into overlapping segments, each of length τ_{max}. By selecting many overlapping, shorter FWC and PC time series from the full control simulation and varying the cutoff lag τ_{max} between 30 and 35 years, we obtain a spread of estimates for the impulse response function $G(\tau)$. We take the mean of these over the first 30 years as our best guess. To estimate the uncertainty, we combine the standard deviation of all estimates in quadrature with the mean of the uncertainty estimates from each fit.

Finally, we integrate the impulse response function to obtain the FWC climate (or "step") response function:

$$FWC_{step}(t) = \int_0^t G(\tau) \, d\tau \quad \text{where } t \leq \tau_{max} \qquad (3)$$

To reconstruct FWC variability, we use a convolution of the impulse response function G with sea-level pressure variations. We use monthly mean sea-level pressure fields from the European Centre for Medium-Range Weather Forecasting atmospheric reanalysis of the 20th century, ERA-20C (Poli et al., 2016). Although this

product only assimilates surface pressure and marine wind observations, it does a good job, for example, of reproducing the North Atlantic Oscillation (Poli et al., 2016; Weisheimer et al., 2017) and has been used in several recent Arctic studies (e.g., Belleflamme et al., 2015; Close et al., 2017). We compare reconstructed changes in Arctic FWC with observed changes from in situ data (Rabe et al., 2014).

More details concerning the methodology can be found in Kostov et al. (2017, see Appendix), Kostov et al. (2018) and in the supporting information.

3. Seasonal and Interannual FWC Variability

The model's time-mean integrated Arctic FWC is 109,000 km^3 (Figure 1a), which is close to that estimated from recent observations (101,000 km^3; Haine et al., 2015). The amplitude of the seasonal cycle (Figure 1b) is about 10% of this total, in accordance with observations (Serreze et al., 2006) and Coupled Model Intercomparison Project Phase 5 models (Ding et al., 2016). There is a minimum in March and a maximum in September, in antiphase with the freshwater stored as sea ice, as water is exchanged between the two phases over the seasonal cycle with some lost from the Arctic due to ice export. Precipitation minus evaporation, together with river run-off, also contribute to the seasonal cycle, both peaking during the summer, and important principally in localized regions on the shelves (Figure 1d). The same factors are found to determine the seasonal cycle in Arctic FWC in Coupled Model Intercomparison Project Phase 5 models (Ding et al., 2016).

Although the Beaufort Gyre is the largest freshwater reservoir (Figure 1c), the amplitude of the seasonal cycle there is small (Figure 1d), peaking instead around the perimeter of the basin, in keeping with the importance of thermodynamic forcing and source terms. The spatial pattern likely also reflects some redistribution between the interior and shelves, which dominates the variability in steric height on seasonal timescales (Armitage et al., 2016).

Interannual variability in FWC (Figure 1e), however, is largest in the basin interior, suggesting that on these timescales the dynamics of the Beaufort Gyre and the strength of the Transpolar Drift are playing a key role (Niederdrenk et al., 2016). Although the Canada and Makarov Basins, which contain the Beaufort Gyre, represent only 23% of the Arctic's area, the magnitude of the interannual standard deviation of FWC in these basins is 68% of that for the entire Arctic (which is approximately 10,000 km^3, Figure 1a). On these timescales FWC variability in the Beaufort Gyre region is also well-correlated with that for the whole Arctic. Interannual FWC variability is also large north of Svalbard, reflecting variability in the Atlantic inflow and consequent sea-ice edge.

Since FWC variability on seasonal timescales is well-understood and largely associated with a change in phase during ice formation/melt, we remove the seasonal cycle and focus on interannual and longer-term variability. On these timescales Arctic FWC variability is dominated by interior regions of the Arctic where we expect wind-driven ocean dynamics to dominate.

4. Relationship Between Sea-Level Pressure and FWC

The ocean surface stress driving Ekman convergence in the Beaufort Gyre arises due to wind forcing (Proshutinsky et al., 2009), modulated by the sea-ice conditions (e.g., Martin et al., 2014). The details of the momentum transfer through sea-ice are poorly quantified and not fully accounted for in state-of-the-art numerical models (Martin et al., 2016; Tsamados et al., 2014). Here we take the simplest possible approach, as in previous studies (e.g., Morison et al., 2012; Proshutinsky et al., 2009), and consider the relationship between Arctic FWC and sea-level pressure, which is a good proxy for surface winds and whose variability is characterized by its first few EOFs.

Figures 2a–2c show the first three EOFs of sea-level pressure (north of 70°, mean seasonal cycle removed) in the model control run. These three modes of variability explain 50%, 17%, and 13% of the sea-level pressure variance, respectively, (EOF 4 explains < 5%) and are very similar to those calculated from reanalysis data (e.g., Wu et al. (2006)). The first mode projects strongly onto the Arctic Oscillation (Thompson & Wallace, 1998), which has long been thought to be important for Arctic FWC variability through a variety of mechanisms (e.g., Morison et al., 2012; Proshutinsky et al., 2009), while gradients in the second mode align with the Transpolar Drift and hence impact ice and freshwater export from the Arctic through Fram Strait (Tsukernik et al., 2010). In this model the spatial pattern of the third mode is centred over the Canada and Makarov Basins and the associated winds are therefore likely to influence the strength of the Beaufort Gyre.
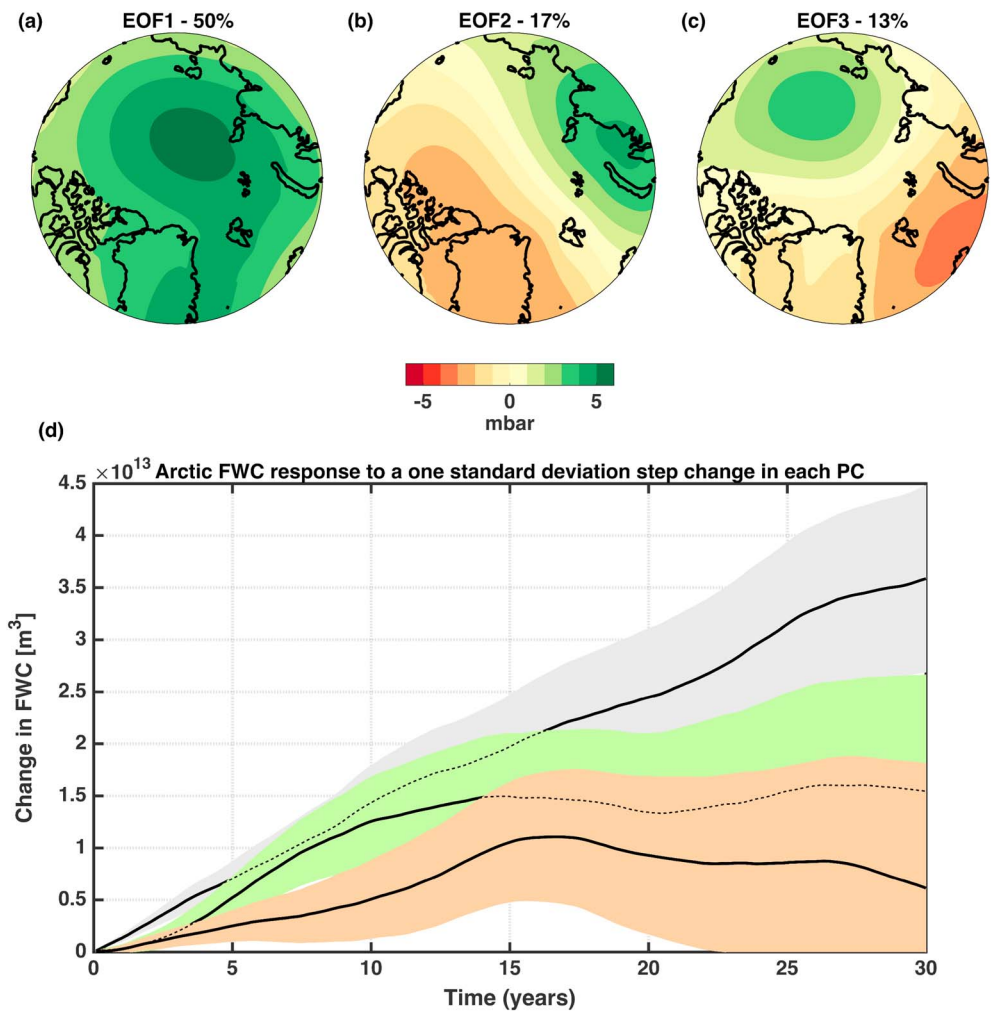
Figure 2. (a–c) First three empirical orthogonal functions (EOFs) of the sea-level pressure north of 70°N (mb). (d) Change in Arctic freshwater content (FWC) in response to a step change of one standard deviation in each of the three principal components of sea-level pressure: PC1 (orange), PC2 (green), and PC3 (grey). Black lines show the mean estimate and shaded envelopes the uncertainty. A step change in sea-level pressure of the magnitude and sign shown in (a)–(c) would result in the change in FWC shown in (d).

Shown in Figure 2d is the response of Arctic FWC to a step change of one standard deviation in each of the three PCs of sea-level pressure (the CRFs). The magnitude of the forcing change in each case is indicated by the amplitude of the EOF patterns in Figures 2a–2c. After a step change in PC1 or PC2, the FWC adjusts to a new equilibrium over 10–20 years. (The response to a step change in PC3 does not appear to level off.) This response is consistent with our expectation that the adjustment timescale of the Beaufort Gyre is decadal, and with the results of step change experiments in ocean-sea-ice models (Marshall et al., 2017).

The interior Arctic Ocean is rather unique in terms of its adjustment processes. Since it is centred on the pole, gradients in the Coriolis parameter are small (Yang et al., 2016) such that Rossby waves are slow and travel around rather than across the basin, rendering them ineffective at communicating change into the interior. Vertical diffusion is small (e.g., Guthrie et al., 2013; Lincoln et al., 2016) due to the sea-ice cover and small tidal amplitude, further hampered by the resulting strong halocline, and there can be no zonally integrated meridional geostrophic flow above the level of the bathymetry. For much of the time (although not all, see Dewey et al., 2018, and Meneghello et al., 2018) the anticyclonic atmospheric circulation results in an anticyclonic surface stress acting on the ocean. In the absence of faster adjustment mechanisms, we might expect changes in the associated surface Ekman layer convergence to steepen isopycnals until eddy generation via baroclinic instability arrests this steepening and allows the system to reach a new equilibrium state. This is indeed what happens in a range of idealized models of the Beaufort Gyre (Davis et al., 2014; Lique et al., 2015; Manucharyan

& Spall, 2016). Simple scaling analysis applied to the volume budget of water above the halocline (see Davis et al., 2014) suggests that the adjustment timescale is decadal and that it is set by the properties of the eddy field. The CRFs shown in Figure 2 indicate that total Arctic FWC in the control run of the coupled climate model HiGEM adjusts to a change in forcing on a similar, decadal timescale.

Since we consider FWC integrated over the entire Arctic, and not just the Beaufort Gyre, other mechanisms clearly also contribute to the long timescale response to a change in sea-level pressure. The large response to a step change in PC2 suggests that the advection of freshwater through Fram and/or Davis Straits via the Transpolar Drift plays an important role (as others have found for shorter timescale variability, e.g., Niederdrenk et al., 2016). Strong and sustained southerly wind stress anomalies over Fram Strait lead to an accumulation of freshwater in the Arctic, while northerlies lead to a draining of the freshwater reservoir. Changes in precipitation minus evaporation over surrounding continents, leading to delayed changes in the freshwater input by river runoff, may also contribute. However, the responses of FWC to a one standard deviation step change in net atmospheric freshwater input (precipitation minus evaporation over the Arctic Ocean plus runoff), and net atmospheric freshwater input to a one standard deviation step change in sea-level pressure, are small (not shown). This suggests that sea-level pressure linked changes in freshwater input from the atmosphere and surrounding continents do not play a large role in this model. A re-partitioning of the freshwater stored as sea ice into the liquid FWC reservoir could also be important. The adjustment of sea-ice volume to a change in the sea-level pressure field is both thermodynamic and dynamic, and involves feedbacks which could introduce long timescales; indeed, the total sea-ice volume in the model control run exhibits some decadal variability (see also Kay et al., 2011). Response functions of total (liquid plus ice) FWC to a step change in PC1 or PC2 exhibit a slightly larger amplitude and slightly longer timescale than those for liquid FWC alone (not shown).

The amplitude of the FWC response to a one standard deviation step increase in any of the first three PCs (Figure 2d) is large ($1 - 4 \times 10^{13}$ m³), one to four times the amplitude of the seasonal cycle in FWC and of the interannual variability in the control run. This is in keeping with the long adjustment timescale; a new equilibrium FWC state is never reached in the control run, because the atmospheric forcing varies on subdecadal timescales throughout. The response to a step change in PC3 is largest; although the third EOF explains much less of the sea-level pressure variance, in this model it projects more strongly onto the strength of the Beaufort High which spins up the Beaufort Gyre.

Note that the response of the FWC to a step change in PC1 or PC2 appears to overshoot its equilibrium value slightly and then oscillate. Although this oscillation is within the uncertainty of our estimate, if physical it could be related to the advection of freshwater recently exported from the Arctic back into the basin after a circuit of the subpolar gyre (Proshutinsky et al., 2015; Stewart & Haine, 2013). In higher resolution models and the real Arctic we might expect a similar oscillation due to eddy memory (Manucharyan et al., 2017), although HiGEM parameterizes rather than resolves eddies at high latitudes so this is unlikely to be important here. A third possibility is exchange between the liquid and solid freshwater reservoirs, resulting from feedbacks on ice formation and melt.

5. Reconstructing FWC Variability

Convolving the model's time history of sea-level pressure with the impulse response function G (equation (2)) for each PC, and then adding the contributions from the three PCs together, allows us to reconstruct a time series of interannual Arctic FWC variability in the control run (Figure 3). The model's total Arctic FWC is well correlated with that reconstructed using PC1 ($R = 0.77$, Figure 3a) and PC2 ($R = 0.82$) such that a reconstructed time series using the first two PCs of sea-level pressure captures almost all of the variability ($R = 0.90$, Figure 3b). Although the model's FWC is also reasonably well correlated with a reconstruction based on PC3 alone ($R = 0.67$), adding the third PC only marginally improves the fit ($R = 0.93$); while the EOFs of sea-level pressure are independent, their impact on the FWC may not be, and it is clear from Figure 3c that the decadal variability in FWC may be overestimated. Nevertheless, the good agreement in Figures 3b and 3c indicates that Arctic FWC variability depends linearly on lagged sea-level pressure and hence that our Green's function methodology is appropriate. Almost all of the interannual variability in FWC in this model control run can be recovered from the sea-level pressure, and it has a memory of at least the previous decade of forcing.

We now attempt to estimate Arctic FWC variations over the last century from atmospheric reanalysis sea-level pressure variations. Convolving the projection of ERA-20C sea-level pressure variability (1900–2011) onto each of the EOFs in Figure 2 with the corresponding impulse response function G, and summing the three
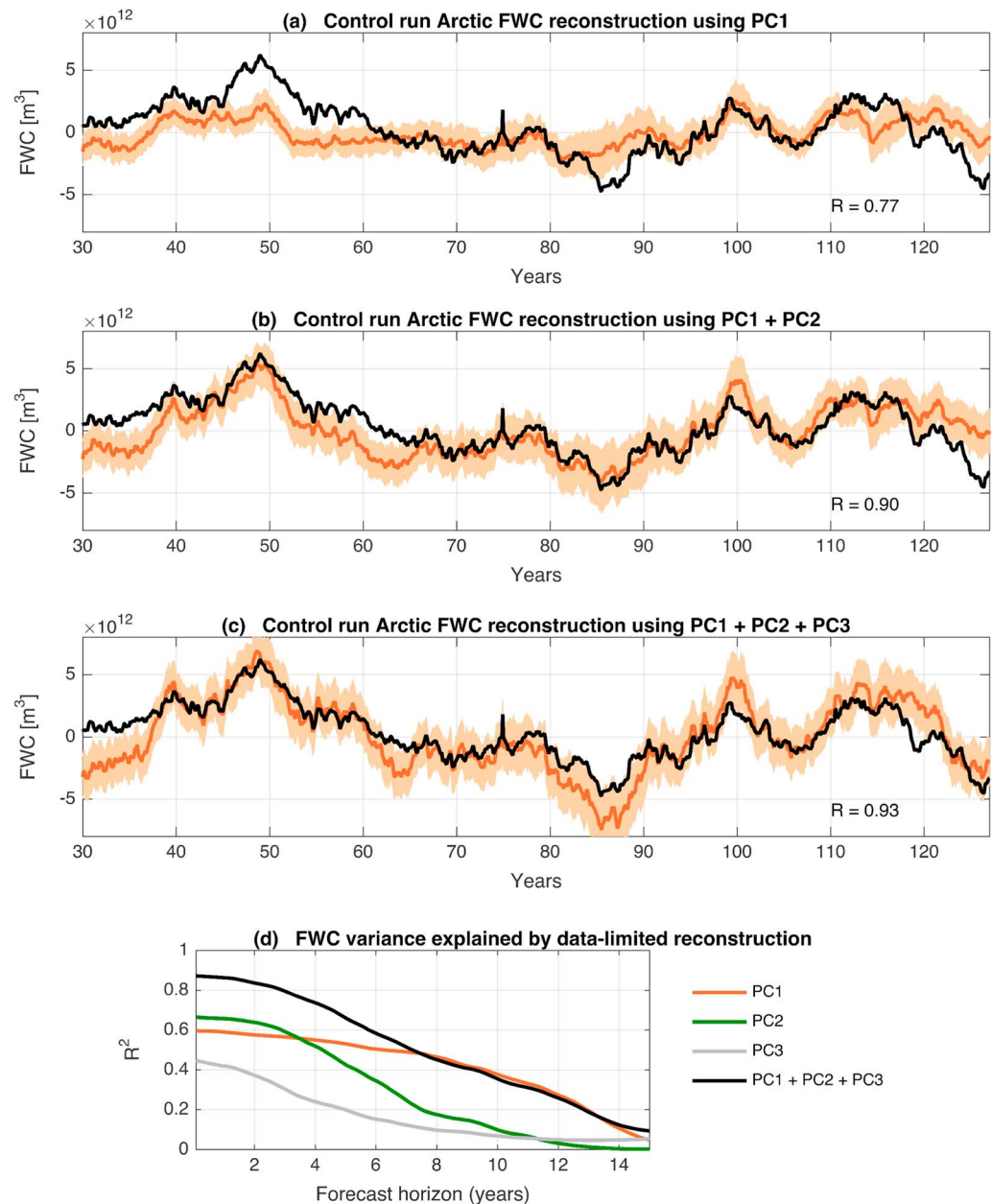
Figure 3. Reconstructed time series of Arctic freshwater content (FWC; orange) in the control run, based on a convolution of the impulse response function with the model sea-level pressure field using (a) PC1 only; (b) PC1 and PC2; and (c) PC1, PC2, and PC3. The model's total (detrended) Arctic FWC is shown in black. Plotted in (d) is the fraction of FWC variance explained (R^2) when the convolution excludes sea-level pressure data from the most recent time period (the forecast horizon).

contributions (orange lines in Figures 4b–4d), results in the FWC time series shown in Figure 4a. (Note that it is only between 1930 and 2011 that the full 30 year response functions are accounted for, and that the FWC anomaly goes to zero by definition in 2041 as the available history of sea-level pressure disappears.) The FWC exhibits pronounced decadal and multidecadal variability of amplitude 10,000 km^3, with sea-level pressure variations projecting onto EOF3 contributing to the longer term variability (Figure 4d) and variations projecting onto EOF1 and EOF2 giving rise to decadal changes (Figures 4b and 4c).

Observed FWC changes between 1992 and 2012 (Rabe et al., 2014) agree very well with the reconstructed time series, despite the significant uncertainties in both. The large increase in FWC during this period can be explained entirely by sea-level pressure variations, via their impact on the sources, sinks and storage of freshwater. The magnitude of the recent increase is comparable to the amplitude of variability in the reconstruction
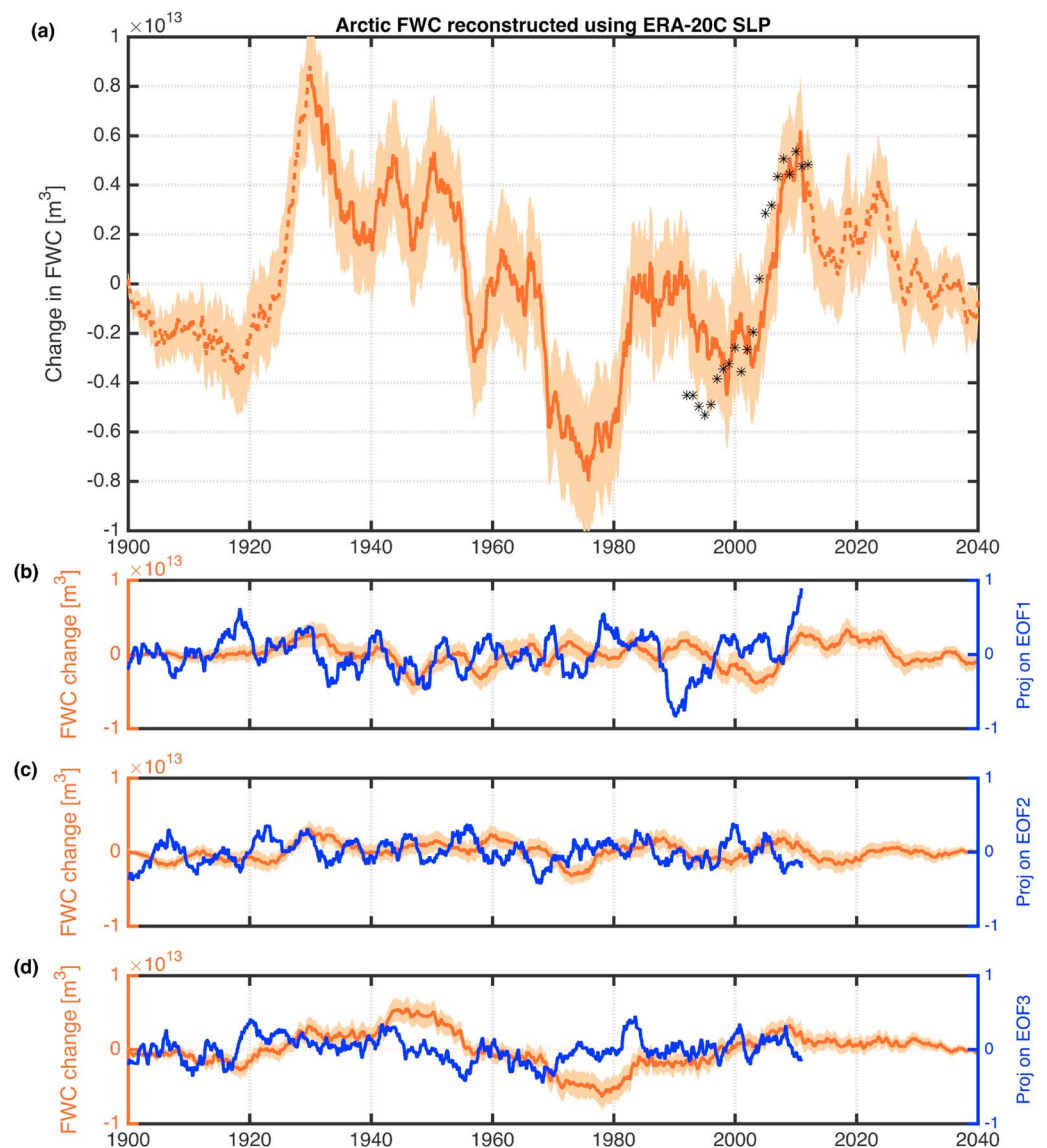
Figure 4. (a) Time series of Arctic freshwater content (FWC; orange) estimated by convolving the projection of ERA-20C sea-level pressure variability onto each of the empirical orthogonal functions (EOFs) in Figure 2 with the corresponding impulse response function *G*, and summing the three contributions. Black stars indicate the observed FWC anomalies in Rabe et al. (2014; who use a different definition of Arctic FWC, relative to a reference salinity of 35 and integrated down to the 34 isohaline over Arctic basins deeper than 500 m). Plotted in blue in (b), (c), and (d) are the projections of the ERA-20C sea-level pressure variability onto EOF1, EOF2, and EOF3, respectively (36-month running means), with their contribution to the FWC time series shown in orange. The time series in (a) is a sum of the orange lines in the other three panels. Note that the uncertainty in all panels reflects only that coming from the the impulse response functions and does not include any contribution from reanalysis sea-level pressure. The dashed orange line in (a) corresponds to periods during which the convolution uses less than the full 30-year response functions.

over the rest of the century. The importance of sea-level pressure, and hence wind-driven ocean dynamics, is consistent with the suggestion from observational data and forced ocean model simulations that changes in the oceanic freshwater import to, and export from, the Arctic may have been partly responsible for the increase in FWC (e.g., Carmack et al., 2016; Rabe et al., 2014).

The large decrease in Arctic FWC during the late 1960s and early 1970s coincides with the time during which a Great Salinity Anomaly propagated around the subpolar North Atlantic (Dickson et al., 1988), suggesting that downstream changes may also have some root in sea-level pressure driven Arctic FWC changes. Note that the 1980s Great Salinity Anomaly was probably not associated with significant Arctic freshwater export (Belkin et al., 1998).

The Arctic FWC's long memory of sea-level pressure changes provides some predictability. Figure 3d shows the correlation (R^2) between model and reconstructed FWC when the convolution excludes sea-level pressure data from the most recent months. The number of months excluded is equivalent to the forecast horizon, that is, the interval of time between the end of the available forcing data and the predicted FWC value. When all three principal components are included in the convolution, a reconstruction from sea-level pressure can still capture half of the interannual variability in FWC in this model when predicting 7 years ahead. This suggests that the stabilization of FWC since 2008 evident in Figure 4 (and consistent with Zhang et al., 2016), and the decrease since then, may be robust.

6. Concluding Discussion

Through lagged multiple linear regression, we have shown that Arctic Ocean FWC in a fully coupled climate model has a memory of sea-level pressure going back more than a decade. This long response timescale is in accordance with our expectations from theory and very idealized numerical models of the Beaufort Gyre (e.g., Davis et al., 2014; Manucharyan et al., 2016). Our results suggest that a similar decadal adjustment timescale applies to FWC integrated over the entire Arctic basin in a more realistic system, with additional complexity introduced by bathymetry, sea-ice, and atmosphere-ocean coupled processes. The decadal timescale reflects a combination of the Beaufort Gyre's spin-up time and the influence of wind-driven sources and sinks of freshwater through the Arctic's gateways.

As a result of the long memory of atmospheric forcing, attribution of changes in Arctic FWC is challenging; while FWC starts to react immediately to a change in sea-level pressure, a new equilibrium is not often reached because the forcing generally exhibits higher frequency variability. It follows that persistent atmospheric forcing has the biggest effect. It is only by convolving the forcing with the response function that we can understand the cause of past FWC variability. Between 1992 and 2012, the Arctic accumulated 12,000 km³ of fresh water (Giles et al., 2012; Rabe et al., 2014); during this period sea-level pressure changes projecting onto EOF3 dominated initially, with changes projecting onto EOF1 only contributing from about 2003.

The long adjustment timescale for Arctic FWC may impact the export of freshwater into the Atlantic, although the link between freshwater accumulation in the Beaufort Gyre and export from the basin is poorly pinned down (Rabe et al., 2013; Wang et al., 2016). There is considerable exchange between the Arctic interior and Siberian shelves (Armitage et al., 2016), such that a relaxation of the gyre need not imply export from the basin. We defer investigation of the redistribution of freshwater within the Arctic basin to a future study. Local forcing within the Arctic's gateways is also important for the freshwater export fluxes (e.g., Curry et al., 2011; Houssais & Herbaut, 2011).

While the details of the response functions illustrated in Figure 2 may well be model dependent, we expect the decadal memory of sea-level pressure to be robust. Neither the adjustment timescale nor the success of the FWC reconstructions in Figures 3 and 4 are sensitive to the details of our analysis method (e.g., area over which the EOFs are calculated, maximum cutoff lag τ_{max}, FWC definition). Ocean-only models forced with a step change in sea-level pressure over the Beaufort Gyre exhibit a similar response (e.g., Marshall et al., 2017).

Our results suggest that changes in Arctic FWC may well be predictable for several years ahead, potentially providing valuable early warning of any significant change in freshwater export to the North Atlantic.

One might ask how robust the relationship between sea-level pressure and Arctic FWC is likely to be in the future. Since sea-ice influences the transfer of momentum from the atmosphere to the ocean, determining the ocean surface stress, as the sea-ice conditions continue to change there is no reason to expect that the same linear relationship between sea-level pressure variations and FWC will hold. In addition, changes in source terms such as runoff, freshwater from ice melt, and precipitation minus evaporation may play a larger role. Although the FWC changes observed to date appear to have resulted from natural atmospheric variability, this may not continue to be the case.

References

Aagaard, K., & Carmack, E. (1989). The role of sea ice and other fresh water in the Arctic circulation. *Journal of Geophysical Research*, *94*, 14,485–14,498.

Armitage, T. W. K., Bacon, S., Ridout, A. L., Thomas, S. F., Aksenov, Y., & Wingham, D. J. (2016). Arctic sea surface height variability and change from satellite radar altimetry and GRACE, 2003-2014. *Journal of Geophysical Research: Oceans*, *121*, 4303–4322. https://doi.org/10.1002/2015JC011579

Belkin, I. M, Levitus, S., Antonov, J., & Malmberg, S. A. (1998). "Great Salinity Anomalies" in the North Atlantic. *Journal of Physical Oceanography*, *41*, 1–68.

Belleflamme, A., Fettweis, X., & Erpicum, M. (2015). Recent summer Arctic atmospheric circulation anomalies in a historical perspective. *The Cryosphere*, *9*(1), 53–64. https://doi.org/10.5194/tc-9-53-2015

Boyer, T., Levitus, S., Garcia, H., Locarnini, R. A., Stephens, C., & Antonov, J. (2005). Objective analyses of annual, seasonal, and monthly temperature and salinity for the World Ocean on a 0.25° grid. *International Journal of Climatology*, *25*, 931–945. https://doi.org/10.1002/joc.1173

Carmack, E. C., Yamamoto-Kawai, M., Haine, T. W. N., Bacon, S., Bluhm, B. A., Lique, C., et al. (2016). Freshwater and its role in the Arctic Marine System: Sources, disposition, storage, export, and physical and biogeochemical consequences in the Arctic and global oceans. *Journal of Geophysical Research: Biogeosciences*, *121*, 675–717. https://doi.org/10.1002/2015JG003140

Close, S., Houssais, M.-N., & Herbaut, C. (2017). The Arctic winter sea ice quadrupole revisited. *Journal of Climate*, *30*(9), 3157–3167. https://doi.org/10.1175/JCLI-D-16-0506.1

Curry, B., Lee, C. M., & Petrie, B. (2011). Volume, freshwater, and heat fluxes through Davis Strait, 2004-05. *Journal of Physical Oceanography*, *41*, 429–436. https://doi.org/10.1175/2010JPO4536.1

Davis, P. E. D., Lique, C., & Johnson, H. L. (2014). On the link between Arctic sea ice decline and the freshwater content of the Beaufort Gyre: Insights from a simple process model. *Journal of Climate*, *27*, 8170–8184. https://doi.org/10.1175/JCLI-D-14-00090.1

Dewey, S., Morison, J., Kwok, R., Dickinson, S., Morison, D., & Andersen, R. (2018). Arctic ice-ocean coupling and gyre equilibration observed with remote sensing. *Geophysical Research Letters*, *45*, 1499–1508. https://doi.org/10.1002/2017GL076229

Dickson, R. R., Meincke, J., Malmberg, S. A., & Lee, A. J. (1988). The Great Salinity Anomaly in the North Atlantic. *Nature*, *256*(5517), 479–482.

Ding, Y., Carton, J. A., Chepurin, G. A., Steele, M., & Hakkinen, S. (2016). Seasonal heat and freshwater cycles in the Arctic Ocean in CMIP5 coupled models. *Journal of Geophysical Research: Oceans*, *121*, 2043–2057. https://doi.org/10.1002/2015JC011124

Gent, P. R., & McWilliams, J. C. (1990). Isopycnal mixing in ocean circulation models. *Journal of Physical Oceanography*, *20*, 150–160. https://doi.org/10.1175/1520-0485

Giles, K. A., Laxon, S. W., Ridout, A. L., Wingham, D. J., & Bacon, S. (2012). Western Arctic Ocean freshwater storage increased by wind-driven spin-up of the Beaufort Gyre. *Nature Geoscience*, *5*, 194–197. https://doi.org/10.1038/ngeo1379

Griffies, S. M., Gnanadesikan, A., Pacanowski, R. C., Larichev, V. D., Dukowicz, J. K., & Smith, R. D. (1998). Isoneutral diffusion in a z-coordinate ocean model. *Journal of Physical Oceanography*, *28*, 805–830. https://doi.org/10.1175/1520-0485

Guthrie, J. D., Morison, J. H., & Fer, I. (2013). Revisiting internal waves and mixing in the Arctic Ocean. *Journal of Geophysical Research: Oceans*, *118*, 3966–3977. https://doi.org/10.1002/jgrc.20294

Haine, T. W, Curry, B., Gerdes, R, Hansen, E., Karcher, M., Lee, C., et al. (2015). Arctic freshwater export: Status, mechanisms, and prospects. *Global and Planetary Change*, *125*, 13–35. https://doi.org/10.1016/j.gloplacha.2014. 11.013

Hasselmann, K., Sausen, R., Maier-Reimer, E., & Voss, R. (1993). On the cold start problem in transient simulations with coupled atmosphere-ocean models. *Climate Dynamics*, *9*(2), 53–61. https://doi.org/10.1007/BF00210008

Houssais, M.-N., & Herbaut, C. (2011). Atmospheric forcing on the Canadian Arctic Archipelago freshwater outflow and implications for the Labrador Sea variability. *Journal of Geophysical Research*, *116*, C00D02. https://doi.org/10. 1029/2010JC006323

Hunke, E. C., & Dukowicz, J. K. (1997). An elastic viscous plastic model for sea ice dynamics. *Journal of Physical Oceanography*, *27*, 1849. https://doi.org/10.1175/1520-0485

IPCC (2013). *Climate change 2013 - The Physical Science Basis. Contribution of Working Group I to the Fourth Assessment Report of the Intergovernmental Panel on Climate Change* (p. 1250). Cambridge, United Kingdom and New York: Cambridge University Press.

Jahn, A., & Holland, M. M. (2013). Implications of Arctic sea ice changes for North Atlantic deep convection and the meridional overturning circulation in CCSM4-CMIP5 simulations. *Geophysical Research Letters*, *40*, 1206–1211. https://doi.org/10.1002/grl.50183

Jahn, A., Tremblay, B., Mysak, L. A., & Newton, R. (2010). Effect of the large-scale atmospheric circulation on the variability of the Arctic Ocean freshwater export. *Climate Dynamics*, *34*, 201–222. https://doi.org/10.1007/s00382-009-0558-z

Johns, T. C., Durman, C. F., Banks, H. T., Roberts, M. J., McLaren, A. J., Ridley, J. K., et al. (2006). The new Hadley Centre Climate Model (HadGEM1): Evaluation of coupled simulations. *Journal of Climate*, *19*, 1327. https://doi.org/10.1175/JCLI3712.1

Kay, J. E., Holland, M. M., & Jahn, A. (2011). Inter-annual to multi-decadal Arctic sea ice extent trends in a warming world. *Geophysical Research Letters*, *38*, L15708. https://doi.org/10.1029/2011GL048008

Kostov, Y., Marshall, J., Hausmann, U., Armour, K. C., Ferreira, D., & Holland, M. M. (2017). Fast and slow responses of Southern Ocean sea surface temperature to SAM in coupled climate models. *Climate Dynamics*, *48*(5), 1595–1609. https://doi.org/10.1007/s00382-016-3162-z

Kostov, Y., Ferreira, D., Armour, K. C., & Marshall, J. (2018). Contributions of greenhouse gas forcing and the Southern Annular Mode to historical Southern Ocean surface temperature trends. *Geophysical Research Letters*, *45*, 1086–1097. https://doi.org/10.1002/2017GL074964

Lincoln, B. J., Rippeth, T. P., Lenn, Y.-D., Timmermans, M. L., Williams, W. J., & Bacon, S. (2016). Wind-driven mixing at intermediate depths in an ice-free Arctic Ocean. *Geophysical Research Letters*, *43*, 9749–9756. https://doi.org/10.1002/2016GL070454

Lique, C., Johnson, H. L., & Davis, P. E. D. (2015). On the interplay between the circulation in the surface and the intermediate layers of the Arctic Ocean. *Journal of Physical Oceanography*, *45*, 1393–1409. https://doi.org/10.1175/JPO-D-14-0183.1

Lique, C., Johnson, H. L., & Plancherel, Y. (2017). Emergence of deep convection in the Arctic Ocean under a warming climate. *Climate Dynamics*, *50*, 3833–3847. https://doi.org/10.1007/s00382-017-3849-9

Lique, C., Treguier, A. M., Scheinert, M., & Penduff, T. (2009). A model-based study of ice and freshwater transport variability along both sides of Greenland. *Climate Dynamics*, *33*, 685–705. https://doi.org/10.1007/s0038200805107

Manucharyan, G. E., & Spall, M. A. (2016). Wind-driven freshwater buildup and release in the Beaufort Gyre constrained by mesoscale eddies. *Geophysical Research Letters*, *43*, 273–282. https://doi.org/10.1002/2015GL065957

Manucharyan, G. E., Spall, M. A., & Thompson, A. F. (2016). A theory of the wind-driven Beaufort Gyre variability. *Journal of Physical Oceanography*, *46*(11), 3263–3278. https://doi.org/10.1175/JPO-D-16-0091.1

Manucharyan, G. E., Thompson, A. F., & Spall, M. A. (2017). Eddy memory mode of multidecadal variability in residual-mean ocean circulations with application to the Beaufort Gyre. *Journal of Physical Oceanography*, *47*(4), 855–866. https://doi.org/10.1175/JPO-D-16-0194.1

Marshall, J., Scott, J., & Proshutinsky, A. (2017). 'Climate Response Functions' for the Arctic Ocean: a proposed coordinated modeling experiment. *Geoscientific Model Development*, *10*, 2833–2848.

Martin, T., Steele, M., & Zhang, J. (2014). Seasonality and long-term trend of Arctic Ocean surface stress in a model. *Journal of Geophysical Research: Oceans*, *119*, 1723–1738. https://doi.org/10.1002/2013JC009425

Martin, T., Tsamados, M., Schroeder, D., & Feltham, D. L. (2016). The impact of variable sea ice roughness on changes in Arctic Ocean surface stress: A model study. *Journal of Geophysical Research: Oceans*, *121*, 1931–1952. https://doi.org/10.1002/2015JC011186

Meneghello, G., Marshall, J., Timmermans, M.-L., & Scott, J. (2018). Observations of seasonal upwelling and downwelling in the Beaufort Sea mediated by sea ice. *Journal of Physical Oceanography, 48*, 795–805. https://doi.org/10.1175/JPO-D-17-0188.1

Morison, J., Kwok, R., Peralta-Ferriz, C., Alkire, M., Rigor, I., Andersen, R., & Steele, M. (2012). Changing Arctic Ocean freshwater pathways. *Nature*, *481*, 66–70. https://doi.org/10.1038/nature10705

Niederdrenk, A. L., Sein, D. V., & Mikolajewicz, U. (2016). Interannual variability of the Arctic freshwater cycle in the second half of the twentieth century in a regionally coupled climate model. *Climate Dynamics*, *47*(12), 3883–3900. https://doi.org/10.1007/s00382-016-3047-1

Poli, P., Hersbach, H., Dee, D. P., Berrisford, P., Simmons, A. J., Vitart, F., et al. (2016). ERA-20C: An Atmospheric Reanalysis of the Twentieth Century. *Journal of Climate*, *29*(11), 4083–4097. https://doi.org/10.1175/JCLI-D-15-0556.1

Proshutinsky, A., Dukhovskoy, D., Timmermans, M.-L., Krishfield, R., & Bamber, J. L. (2015). Arctic circulation regimes. *Philosophical Transactions of the Royal Society of London A: Mathematical, Physical and Engineering Sciences*, *373*(2052), 20140160. https://doi.org/10.1098/rsta.2014.0160

Proshutinsky, A. Y., & Johnson, M. A. (1997). Two circulation regimes of the wind-driven Arctic Ocean. *Journal of Geophysical Research*, *102*, 12,493–12,514.

Proshutinsky, A., Krishfield, R., Timmermans, M.-L., Toole, J., Carmack, E., McLaughlin, F., et al. (2009). Beaufort Gyre freshwater reservoir: State and variability from observations. *Journal of Geophysical Research*, *114*, C00A10. https://doi.org/10.1029/2008JC005104

Rabe, B., Dodd, P. A., Hansen, E., Falck, E., Schauer, U., Mackensen, A., et al. (2013). Liquid export of Arctic freshwater components through the Fram Strait 1998-2011. *Ocean Science*, *9*(1), 91–109. https://doi.org/10.5194/os-9-91-2013

Rabe, B., Karcher, M., Kauker, F., Schauer, U., Toole, J. M., Krishfield, R. A., et al. (2014). Arctic Ocean basin liquid freshwater storage trend 1992-2012. *Geophysical Research Letters*, *41*, 961–968. https://doi.org/10.1002/2013GL058121

Roberts, M., & Marshall, D. (1998). Do we require adiabatic dissipation schemes in eddy-resolving ocean models? *Journal of Physical Oceanography*, *28*, 2050–2063. https://doi.org/10.1175/1520-0485

Serreze, M. C., Barrett, A. P., Slater, A. G., Woodgate, R. A., Lammers, R. B., Steele, M., et al. (2006). The large-scale freshwater cycle of the Arctic. *Journal of Geophysical Research*, *111*, C11010. https://doi.org/10.1029/2005JC003424

Shaffrey, L. C., Stevens, I., Norton, W. A., Roberts, M. J., Vidale, P. L., Harle, J. D., et al. (2009). U.K. HiGEM: The new U.K. High-Resolution Global Environment Model—Model description and basic evaluation. *Journal of Climate*, *22*, 1861. https://doi.org/10.1175/2008JCLI2508.1

Stewart, K. D., & Haine, T. W. N. (2013). Wind-driven Arctic freshwater anomalies. *Geophysical Research Letters*, *40*, 6196–6201. https://doi.org/10.1002/2013GL058247

Stouffer, R. J., Yin, J., Gregory, J. M., Dixon, K. W., Spelman, M. J., Hurlin, W., et al. (2006). Investigating the causes of the response of the thermohaline circulation to past and future climate changes. *Journal of Climate*, *19*(8), 1365–1387. https://doi.org/10.1175/JCLI3689.1

Thompson, D. W. J., & Wallace, J. M. (1998). The Arctic Oscillation signature in the wintertime geopotential height and temperature fields. *Geophysical Research Letters*, *25*, 1297–1300.

Tsamados, M., Feltham, D. L., Schroeder, D., Flocco, D., Farrell, S. L., Kurtz, N., et al. (2014). Impact of variable atmospheric and oceanic form drag on simulations of Arctic sea ice. *Journal of Physical Oceanography*, *44*, 1329–1353. https://doi.org/10.1175/JPO-D-13-0215.1

Tsukernik, M., Deser, C., Alexander, M., & Tomas, R. (2010). Atmospheric forcing of Fram Strait sea ice export: a closer look. *Climate Dynamics*. https://doi.org/10.1007/s00382-009-0647-z

Vihma, T. (2014). Effects of Arctic sea ice decline on weather and climate: A review. *Surveys in Geophysics*, *35*(5), 1175–1214. https://doi.org/10.1007/s10712-014-9284-0

Wang, Q., Ilicak, M., Gerdes, R., Drange, H., Aksenov, Y., Bailey, D. A., et al. (2016). An assessment of the Arctic Ocean in a suite of interannual CORE-II simulations. Part I: Sea ice and solid freshwater. *Ocean Modelling*, *99*, 110–132. https://doi.org/10.1016/j.ocemod.2015.12.008

Weisheimer, A., Schaller, N., O'Reilly, C., MacLeod, D. A., & Palmer, T. (2017). Atmospheric seasonal forecasts of the twentieth century: Multi-decadal variability in predictive skill of the winter North Atlantic Oscillation (NAO) and their potential value for extreme event attribution. *Quarterly Journal of the Royal Meteorological Society*, *143*(703), 917–926. https://doi.org/10.1002/qj.2976

Wu, B., Wang, J., & Walsh, J. E. (2006). Dipole anomaly in the winter Arctic atmosphere and its association with sea ice motion. *Journal of Climate*, *19*(2), 210–225. https://doi.org/10.1175/JCLI3619.1

Yang, J., Proshutinsky, A., & Lin, X. (2016). Dynamics of an idealized Beaufort Gyre: 1. The effect of a small beta and lack of western boundaries. *Journal of Geophysical Research: Oceans*, *121*, 1249–1261. https://doi.org/10.1002/2015JC011296

Zhang, J., Steele, M., Runciman, K., Dewey, S., Morison, J., Lee, C., et al. (2016). The Beaufort Gyre intensification and stabilization: A model-observation synthesis. *Journal of Geophysical Research: Oceans*, *121*, 7933–7952. https://doi.org/10.1002/2016JC012196

Zhao, M., Timmermans, M.-L., Cole, S., Krishfield, R., & Toole, J. (2016). Evolution of the eddy field in the Arctic Ocean's Canada Basin, 2005-2015. *Geophysical Research Letters*, *43*, 8106–8114. https://doi.org/10.1002/2016GL069671